STABILITY ANALYSIS OF SEAFLOOR FOUNDATIONS

TOKUO YAMAMOTO, Ph.D., Associate Professor
Ocean Engineering Division, Rosenstiel School of Marine and Atmospheric Science, University of Miami, 4600 Rickenbacker Causeway, Virginia Key, Miami, Florida 33149, U.S.A.

and

YASUMASA SUZUKI, Research Engineer
Port and Harbour Research Institute
Ministry of Transport
Yokosuka, Japan

ABSTRACT

Stability analysis of homogeneous and inhomogeneous seabed foundations under attack by storm waves are made by calculating the wave induced effective stresses. Wave induced effective stress analysis of homogeneous seabed is made using the theory previously developed by the senior author which is based on the poro-elastic theory by Biot. Effective stresses in inhomogeneous seabeds induced by waves are calculated by approximating an inhomogeneous bed by many layers of homogeneous soils each of which has different geotechnical properties of soils. A good agreement is obtained between the theory and the pore pressure data in situ field measurements. For a given wave length, it is found that there exists a most unstable thickness of homogeneous seabed when the seabed thickness is one-fifth of the wave length. As a realistic example of an inhomogeneous bed, the effective stresses in a typical seabed formation at the Mississippi Delta area of the Gulf of Mexico under the attack of design storm waves are calculated. The numerical results indicate that the storm waves induce a continuous submarine landslide which extends as deep as 9 m from the mud line. Numerical calculations also indicate that such landslides and liquefaction of seabeds can be prevented by placing a layer of concrete blocks or rubbles on the top of the seabeds.

INTRODUCTION

As ocean waves propagate over the continental shelf, turbulent boundary layers developed on the mud line and submarine sediment deposits experience wave-induced pore pressure and effective stresses. Consequently the wave energy is dissipated by the turbulence in the boundary layers, percolations and soil internal frictions in the seabed and the seabed is disturbed by the wave induced effective stresses. Because overall wave-seabed interaction is rather complicated, only the wave induced effective stresses and pore pressures are considered in this paper. The problem of the wave damping due to the turbulent boundary layers, percolations and internal friction of seabed soils is out of the scope of this paper.

If the wave induced effective stress state in the submarine soils exceed the limit equilibrium, the seabeds will fail and may result in the liquefaction and submarine landslides. Such wave induced liquefaction and slide of seafloor foundations are evidenced as the flotation of buried pipelines at Australia coasts, the uneven settlements of gravity-type oil drilling rigs at North Sea and toppling of several jacket-type oil drilling rigs and numerous pipeline failures at the Mississippi Delta area.

The senior author has solved the effective stress state in homogeneous and isotropic seabeds induced by ocean waves based on the Biot's (1941) three-dimensional consolidation theory (Yamamoto, 1977). An almost identical theory was later published by Madsen (1978) except he assumed unisotropic soil permeabilities while assuming an isotropical elasticity of the soil. However, as pointed out by Biot (1955) such assumption is physically inconsistent. Mei and Foda (1980) developed the so-called boundary layer method approximating Yamamoto's (1977) exact solution which considerably simplify the numerical calculations. The theory by Yamamoto (1977) has been substantiated by a laboratory experimentation (Yamamoto, et al., 1978). Further verification of the theory is made in this paper by comparing the theory with the pore pressure data from in situ measurements in fine-grained sediment bed at the Mississippi Delta area by Bennett and Faris (1979).

The real seabeds on the continental shelves are usually not homogeneous but the geotechnical properties of soils vary with the distance from the sea-seabed interface or the mud line. The purpose of this paper is to extend the existing theory by the author for the homogeneous seabeds to more realistic inhomogeneous seabeds. An inhomogeneous seabed is approximated by many layers of homogeneous soils each of which has different values of geotechnical properties and the thickness of the sublayers. Seed and Rahman (1978) computed the wave induced pore pressures in a multi-layered seabed assuming that soils are rigid and pore water is incompressible. However such solution is only applicable to very permeable seabeds as pointed out by Yamamoto (1978). Furthermore, their theory provides no information on wave induced effective stresses in ses-bed which are provided by the present theory.

As illustrative examples, the typical seabed formations at the North Sea and the Mississippi Delta area under attack of design storm waves are analyzed. The results indicate high potenetial of massive landslide and liquefaction of submarine seabed foundation. The numerical calculations suggest that such liquefactions and landslides of seabed can be prevented by placing a layer of concrete blocks or rubbles on the top of the seabeds.

PORO-ELASTIC THEORY FOR MULTI-LAYERED SEABEDS RESPONSE TO WATER WAVES

An inhomogeneous seabed is approximated by many layers of homogeneous soils each of which has different values of geotechnical properties and thicknesses. Figure 1 shows a definition sketch of a two-dimensional water wave propagating over a multi-layered seabed. The wave propagates from right to left. The x-axis is taken on the mud line and the positive z-axis is taken downward from the mud line. Soils in each sublayer of seabed are assumed to response linearelastically to waves. Assuming that displacements of soils and pore water are relatively small, the inertia of soils and pore water are neglected. For soft clays, the inertia terms may not be negligibly small as indicated by Dawson (1978). Nonetheless, the error due to neglection of the inertia terms is considered to be small compared to the errors due to the uncertainty of geotechnical properties of submarine soils. The results including the inertia terms will be published in a future paper.

The continuity equation is given as,

$$\frac{k_j}{\gamma_j} \nabla^2 p_j = \frac{n_j}{K'_j} \frac{\partial p_j}{\partial t} + \frac{\partial \varepsilon_j}{\partial t} \quad (j = 1,2, ---,N) \tag{1}$$

where p_j is the excess pore-water pressure, ε_j is the volume strain of the porous medium, t is the time, k_j is the coefficient of permeability of the soil, γ_j is the unit weight of the pore-water, n_j is the porosity, and K'_j is the apparent bulk modulus of pore-water. The subscript j indicates the j - th layer and N is the total number of layers. The volume strain of the soil matrix for the two-dimensional problem is

$$\varepsilon_j = \frac{\partial u_j}{\partial x} + \frac{\partial w_j}{\partial z} \tag{2}$$

where u_j is the horizontal component of soil displacement and w_j is the vertical component of soil displacement.

From the effective stress concept and Hooke's law, the equation of equilibrium is

$$G_j \nabla^2 u_j + \frac{G_j}{1-2\nu_j} \frac{\partial \varepsilon_j}{\partial x} = \frac{\partial p_j}{\partial x} \tag{3}$$

$$G_j \nabla^2 w_j + \frac{G_j}{1-2\nu_j} \frac{\partial \varepsilon_j}{\partial z} = \frac{\partial p_j}{\partial z} \tag{4}$$

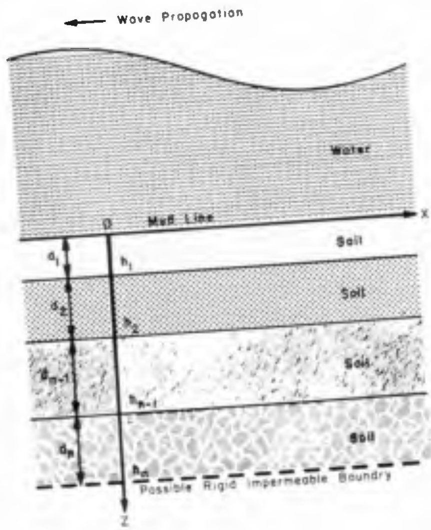

Figure 1. The definition sketch of a multi-layered seabed.

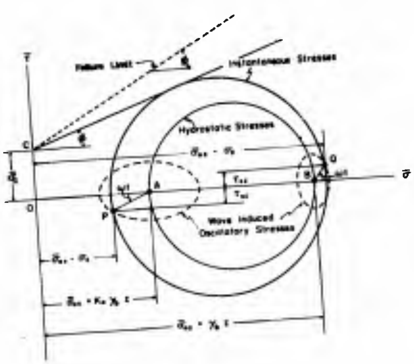

Figure 2. The Mohr's circle diagram of wave induced effective stresses.

where G_j is the shear modulus of the soil, and ν_j is Poisson's ratio for the soil.

Equations (1), (3) and (4) from the governing equations of the pore-water and the soils to be solved for p_j, u_j and w_j.

The effective stresses are related to the strains by Hooke's law as

$$\left(\sigma'_x\right)_j = 2G_j \left[\frac{\partial u_j}{\partial x} + \frac{\nu_j}{1 - 2\nu_j} \varepsilon_j\right] \tag{5}$$

$$\left(\sigma'_z\right)_j = 2G_j \left[\frac{\partial w_j}{\partial z} + \frac{\nu_j}{1 - 2\nu_j} \varepsilon_j\right] \tag{6}$$

$$\left(\tau'_{xz}\right)_j = G_j \left[\frac{\partial u_j}{\partial z} + \frac{\partial w_j}{\partial x}\right] \tag{7}$$

wherein $(\sigma'_x)_j$ is the effective normal stress in the x-direction, $(\sigma'_z)_j$ is the effective normal stress in the z-direction, and $(\tau'_{xz})_j$ is the shear stress in the z-direction on the plane perpendicular to the x-axis.

In the case of a sinusoidal wave propagating over the seabed, the response of the seabed to the wave is considered to be periodic in both time and space. Then, it is reasonable to assume that p_j, u_j and w_j are also periodic in time and space, or

$$p_j = p_j(z) \exp(i\theta) \tag{8}$$

$$u_j = U(z) \exp(i\theta) \tag{9}$$

$$w_j = W(z) \exp(i\theta) \tag{10}$$

where,

$$\theta = \lambda x + \omega t \tag{11}$$

λ is the wave number, ω is the angular wave frequency, and i is the imaginary unit ($i^2 = -1$). The right hand sides of Eqs. (8), (9) and (10) are complex. U_j, w_j and P_j are the function of z only.

Substituting Eqs. (9), (19) and (10) into the governing Eqs. (1), (3) and (4), the three simultaneous ordinary differential equations of second order can be obtained. The differential equations are linear and homogeneous and the characteristic equation is given as:

$$(D^2 - \lambda^2)^2 (D^2 - \lambda_j'^2) = 0 \tag{12}$$

where D is the operator, d/dz, and λ_j' is given as

$$\lambda_j'^2 = \lambda^2 + i \frac{\gamma_j}{k_j}\omega\left[\frac{n_j}{K'} + \frac{(1-2\nu_j)}{2(1-\nu_j)G_j}\right] \tag{13}$$

From Eq. (12) the general solutions of U_j, W_j and P_j are:

$$U_j = a_{ij}\exp[\lambda z] + a_{2j}\exp[-\lambda z] + a_{3j}\frac{z}{h_j}\exp[\lambda z] + a_{4j}\frac{z}{h_j}\exp[-\lambda z] + a_{5j}\exp[\lambda_j' z] + a_{6j}\exp[-\lambda_j' z] \tag{14}$$

$$W_j = b_{1j}\exp[\lambda z] + b_{2j}\exp[-\lambda z] + b_{3j}\frac{z}{h_j}\exp[\lambda z] + b_{4j}\frac{z}{h_j}\exp[-\lambda z] + b_{5j}\exp[\lambda_j' z] + b_{6j}\exp[-\lambda_j' z] \tag{15}$$

$$P_j = c_{1j}\exp[\lambda z] + c_{2j}\exp[-\lambda z] + c_{3j}\frac{z}{h_j}\exp[\lambda z] + c_{4j}\frac{z}{h_j}\exp[-\lambda z] + c_{5j}\exp[\lambda_j' z] + c_{6j}\exp[-\lambda_j' z] \tag{16}$$

in which h_j is the depth of the lower boundary of the j - th layer, and a_{mj}, b_{mj} and c_{mj} (m=1, ..., b; j=1, ..., N) are arbitrary constants. However, the coefficients a_{mj}, b_{mj} and c_{mj} are not independent on each other, and the relationship can be obtained from Eqs. (1), (3) and (4) as:

$$\left.\begin{aligned}
b_{1j} &= -ia_{1j} + i(A_{1j}/h_j)a_{3j}\\
b_{2j} &= ia_{2j} + i(A_{1j}/h_j)a_{4j}\\
b_{3j} &= -ia_{3j}\\
b_{4j} &= ia_{4j}\\
b_{5j} &= -i(\lambda_j'/\lambda)a_{5j}\\
b_{6j} &= i(\lambda_j'/\lambda)a_{bj}
\end{aligned}\right\} \tag{17}$$

$$\left.\begin{aligned} c_{1j} &= -\, i(A_{2j}/h_j)a_{3j} \\ c_{2j} &= i(A_{2j}/h_j)a_{4j} \\ c_{3j} &= c_{4j} = 0 \\ c_{5j} &= A_{3j}\, a_{5j} \\ c_{6j} &= A_{3j}\, a_{6j} \end{aligned}\right\} \tag{18}$$

where

$$\begin{aligned} A_{1j} &= \frac{1}{\lambda}\left[1 + \frac{n_jG_j}{K'}\,\frac{3 - 4\nu_j}{1 - 2\nu_j}\right] \Big/ \left[1 + \frac{n_jG_j}{K'}\,\frac{1}{1 - 2\nu_j}\right] \\ A_{2j} &= 2G_j \Big/ \left[1 + \frac{n_jG_j}{K'}\,\frac{1}{1 - 2\nu_j}\right] \\ A_{3j} &= 2\gamma\omega G_j\,(1 + \nu_j)\left[\frac{n_j}{K'} + \frac{1 - 2\nu_j}{2(1 - \nu_j)G_j}\right] \Big/ \left[\lambda k_j\,(1 - 2\nu_j)\right] \end{aligned} \tag{19}$$

Thus, in order to calculate U_j, W_j and P_j, unknown constants a_{1j}, a_{2j}, ..., a_{6j} (j = 1, 2, ..., 6) should be determined in each layer. These 6 x N constants can be determined from boundary conditions at the bed surface, at the interfaces between the sublayers, and at the bottom bed rock boundary.

In general, because of the interaction between the water waves and the seabeds, the properties of the waves will be changed under the influence from the seabeds. In this paper, we assume that the changes of wave properties are negligible, or the relative acceleration between water particles and soils are very small. Therefore, the boundary conditions at the bed surface are that the vertical effective stress is zero, that the shear stress is negligibly small, and that the sinusoidal pressure fluctuation exists, or at $z = 0$.

$$(\sigma_z')_1 = 2G_1\left[\frac{\partial\omega_1}{\partial z} + \frac{\nu_1}{1 - 2\nu_1}\left(\frac{\partial u_1}{\partial x} + \frac{\partial\omega_1}{\partial z}\right)\right] = 0 \tag{20}$$

$$(\tau'_{xz})_1 = G_1\left(\frac{\partial u_1}{\partial z} + \frac{\partial \omega_1}{\partial x}\right) = 0 \tag{21}$$

$$p_1 = p_o \exp(i\theta) \tag{22}$$

where $(\sigma'_z)_1$ is the effective normal stress in the z direction in the first layer, $(\tau_{xz})_1$ is the shear stress in the z direction on the plane perpendicular to the x axis in the first layer, p_1 is the pore-water pressure in the first layer, and p_o is the amplitude of pressure fluctuation at the bed surface.

The boundary conditions at the interfaces between the sublayers are that of the soil stresses, the pore-water pressures, the pore-water flow, and the soil displacement are continuous, of at $z = h_j$:

$$\left.\begin{array}{ll} (\sigma'_z)_j = (\sigma'_z)_{j+1} , & (\tau_{xz})_j = (\tau_{xz})_{j+1} \\ p_j = p_{j+1} , & k_j(\partial p_j/\partial z) = k_{j+1}(\partial p_{j+1}/\partial z) \\ u_j = u_{j+1} , & w_j = w_{j+1} \end{array}\right\} \tag{23}$$

If the lowest layer (N - th layer) is on an impermeable and rigid bed, the boundary conditions are that no soil displacements at the boundary and no flow across the boundary are allowed, or at $z = h_n$:

$$u_N = 0,\ w_N = 0,\ \partial p_N/\partial z = 0 \tag{24}$$

For a semi-infinite half-plane, the boundary conditions may be given as:

$$u_N,\ w_N,\ p_N \to 0 \text{ as } z\ \infty \tag{25}$$

From Eqs. (14), (15), (16), (17) and (18), this means that:

$$a_{1N} = 0,\ a_{3N} = 0,\ a_{5N} = 0 \tag{26}$$

FAILURE ANALYSIS

So far, only the wave induced incremental changes in stresses and pressures in soils from the initial equilibrium state have been considered. In this section the failure mechanisms of soils induced by waves are considered. From this point on, the traditional sign convention for stresses in the soil mechanics will be used, i.e., a stress is positive when it acts as a compression. The subscript j for the effective stresses are omitted for simplicity in the following development.

The total effective stress, $\bar{\sigma}_z$, in the z-direction is given as

$$\bar{\sigma}_z = \bar{\sigma}_{oz} - \sigma'_z \tag{27}$$

where $\bar{\sigma}_{oz}$ = effective normal stress in the z-direction at initial equilibrium and given as:

$$\bar{\sigma}_{oz} = \gamma_b \; z = \gamma(G_s - 1)z \tag{28}$$

where γ_b = buoyant unit weight of the soil, γ = unit weight of water (9800 N/m^3), and G_s = specific gravity of soil grains σ'_z in Eq. (28) is the incremental effective stress given by Eq. (6). The total effective normal stress, $\bar{\sigma}_x$, in x-direction is given by:

$$\bar{\sigma}_x = \bar{\sigma}_{ox} - \sigma'_x \tag{29}$$

where $\bar{\sigma}_{ox}$ is the effective stress at the initial hydrostatic equilibrium and may be given as:

$$\bar{\sigma}_{ox} = K_o \; \bar{\sigma}_{oz} = K_o \; \gamma_b \; z$$

where K_o is the coefficient of earth pressure at rest and is related to the Poisson ratio, ν, as:

$$K_o = \frac{\nu}{1-\nu} \tag{31}$$

σ'_x in Eq. (29) is given by Eq. (5). The values of K_o for soils range from 0.4 to 1.0 (Scott, 1963).

Since the shear stresses on horizontal and vertical planes are zero at the initial equilibrium, the total shear stress, $\bar{\tau}_{xz}$, is related to the incremental shear stress, τ'_{xz}, of Eq. (17) as

$$\bar{\tau}_{xz} = - \bar{\tau}'_{xz} \tag{32}$$

Equations (27), (29) and (32) may be represented by the Mohr's circles as shown in Fig. 2. The Mohr's circle at a given instance is illustrated by a heavy solid circle passing through points P and Q. The point P and Q rotates on the shear ellipses shown by dashed lines at wave angular frequency, ω, as the waves progress over the seabed.

The failure condition for a given soil may be given as

$$\bar{\tau}_f \geq \; \bar{\sigma}_f \tan \phi_f + c \tag{33}$$

where ϕ_f = angle of internal friction of the soil, c = cohesion of the soil, τ_f = shear stress on the failure plane, and $\bar{\sigma}_f$ = effective normal stress on the failure plane. The limiting failure condition given by Eq. (33) is shown by the dashed straight line in Fig. 2.

Let the angle, ϕ, between the tangent to the instantaneous Mohr circle from point C (0,c) and the horizontal in Fig. 2 be defined as the "stress angle." Then the failure criteria of the soil element at a given point at a given instance may be defined as

$$\phi(x,z,t) \geq \phi_f \tag{34}$$

The stress angle, ϕ, is related to the stresses on the vertical and horizontal planes as

$$\frac{\bar{\sigma}_z + \bar{\sigma}_x}{2} \sin\phi + c \cos\phi = \left[\left(\frac{\bar{\sigma}_z - \bar{\sigma}_x}{2}\right)^2 + \bar{\tau}_{xz}^{\,2} \right]^{1/2} \tag{35}$$

COMPARISON BETWEEN THEORY AND FIELD DATA

The pore-elastic theory presented in this paper has been substantiated by laboratory experiments of a coarse sand bed and fine sand bed (Yamamoto, et al., 1978). In order to further verify the theory, the theory is compared with the wave induced pore-pressure data from in situ measurements in the field available in the literature. Bennett and Faris (1979) measured the wave induced pore-pressure in fine-grained submarine sediments at the East Bay area of the Mississippi Delta in 12.5 m of water. They measured the 30 min. time history record of the pore-pressures at 6.3 m and 15.3 m below mud line as well as the bottom pressure. The 30 min long records are divided into three and the average values of the peak to peak pressures are calculated. The significant wave length is 52 m from the linear theory. The geotechnical properties of the sediments are estimated as the shear modulus, $G = 1.0 \times 10^6$ N/m^2, the Poisson ratio, $\nu = 0.333$, the porosity, $n = 0.5$, and the permeability, $k = 1.0 \times 10^{-6}$ m/s. Infinite thickness of a homogeneous isotropic seabed is assumed in the theoretical calculations. Since up to 10% by volume of undesolved gas in the sediments are reported, both saturated case as well as the case of 90% saturation are computed in the numerical calculations. The comparisons between the theory and the field measurements for the ratio, p/p_o, of the amplitude of pore pressure and the amplitude of bottom pressure vs. the depth d are shown in Fig. 3. The field data fall in between the theoretical curves of 90% saturation and 100% saturation. Considering the limited information about the geotechnical properties of these sediments, Fig. 3 shows an excellent agreement between the theory and the field measurements. This agreement supports the credibility of the present theory in some degree.

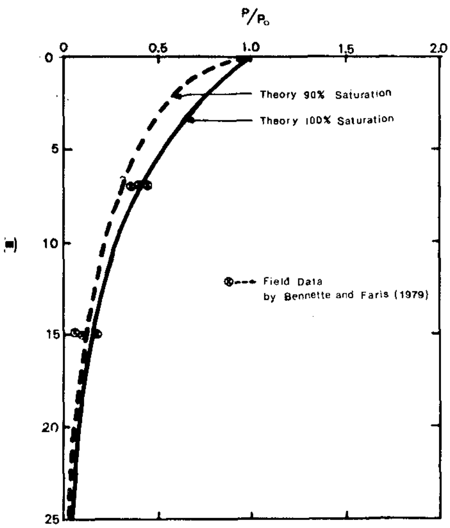

Figure 3. Comparisons between theory and field data of wave induced pore pressures. Data from Bennett and Faris (1979).

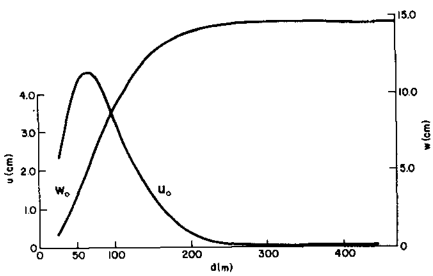

Figure 4. The horizontal displacement, u_o, and the vertical displacement, w_o, of the soil at the mud line vs. the bed thickness, d.

EFFECTS OF THE BED THICKNESS ON THE BED RESPONSE

In order to investigate the effects of the bed thickness on the bed response to waves, a single homogeneous soil bed with varying bed thickness, d, on an impermeable rigid bedrock is first considered. The North Sea design condition of wave characteristics and the geophysical properties of soil is used in calculations; wave period $T = 15$ s, wave length $L = 324$ m, wave height $H = 24$ m, water depth $h = 70$ m, shear modulus $G = 1.0 \times 10^7$ N/m^2, permeability $k = 1.0 \times 10^{-4}$ m/s, porosity $n = 0.3$, Poisson ratio $\nu = 0.333$, cohesive strength $c = 0$ bulk modulus of pore water $K' = 2.3 \times 10^9$ N/m^3. The amplitude of bottom pressure calculated from the linear wave theory is $p_o = 5.60 \times 10^4$ N/m^2.

The plots of the horizontal displacements, u_o, and the vertical displacement, w_o, of the soil at the mud line vs. the bed thickness, d, are shown in Fig. 4. The horizontal displacement u_o first increases as the bed thickness d increases, reaches the maximum value of 4.6 cm at $d = 61.8$ m, then decreases thereafter and vanishes as d tends to infinity. The vertical displacement w_o monotonously increases with d and reaches a constant value of 14.5 cm as d tends to infinity. This suggest that there exists the most unstable bed thickness when $d = 0.20$ L. Figure 5 shows the distribution of stress angle ϕ in the seabed of infinite thickness which is evaluated from Eq. (35) which represents Mohr's effective stress diagram illustrated in Fig. 2. $x = 0$ represents the location of wave crest and $x = 162$ m represents the location of wave trough. Although the distribution of ϕ in the bed is not exactly symmetrical with respect to $x = 0$, it is nearly symmetrical and only the region of a half wavelength is shown in Fig. 5. The wave induced effective stresses are small for this case and the maximum value of $\phi = 27.2^o$ occurs 1.5 m below the mud line under the wave crest. If the failure limit ϕ_f of the soil is 30^o, the bed withstands the wave loading and therefore the bed is stable. Figure 6 shows the distribution of ϕ in the bed if bed thickness $d = 61.8$ m. For this case, the stress state becomes most unstable. Under the wave crest, the stress angle ϕ becomes very large near the mud line. If the failure limits, ϕ_f, of the soil is 30^o, the top portion of the bed as deep as 15 m fails by wave loading. Since the entire bed continuously fails as the wave progresses, the top pertion of bed up to 7 m may be liquefied and result in a continuous landslide if the bed surface has even a slight angle to the horizontal. Therefore, if the footing of an offshore structure is less than 15 m, the structure suffers from an uneven settlement. Pipelines buried shallower than 15 m may float. Since the bed thickness at the North Sea varies from 15 to 80 m, it may be said that the submarine seabed foundation at the North Sea is usually unstable against large storm waves. Some protection work may be needed.

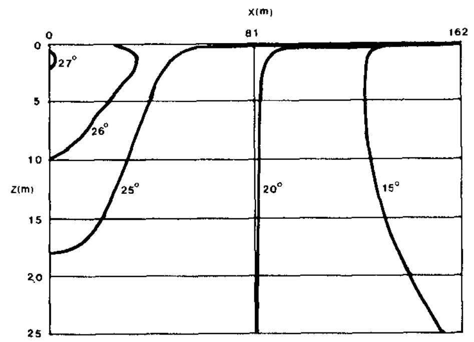

Figure 5. The distribution of the effective stresses in the seabed in terms of stress angle ϕ in degrees for an infinitely thick bed $d = \infty$.

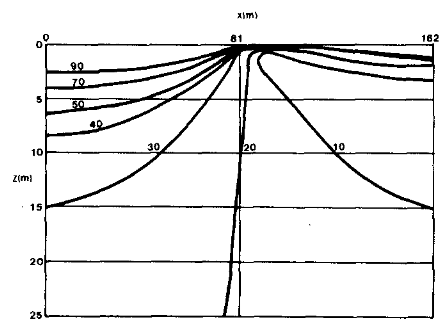

Figure 6. The distribution of the effective stresses in the seabed in terms of stress angle ϕ in degrees for a fine bed thickness $d = 61.8$ m.

RESPONSE OF INHOMOGENEOUS BEDS TO WAVES-STABILITY ANALYSIS OF MISSISSIPPI DELTA CLAY BED WITH "CRUST PROFILE"

As a practical example of inhomogeneous seabeds, the behavior of the seabed at the offshore area surrounding the Mississippi River Delta under attack of a design storm wave is analyzed. A bottom supported platform and numerous buried pipelines were destroyed by massive submarine landslides in this area induced by the storm waves during hurricane "Camille" in 1969 (Bea and Arnold, 1973). The seabed soil formation is characterized by the so-called "crust profile" where a relatively stiff top soil layer and a very weak sublayer exists above a normally consolidated deeper layer. Some of the geotechnical properties of the soils at the area are given in Bea and Arnold (1973). For the numerical calculations, the seabed is subdivided into five layers with different soil properties and thicknesses which approximates the in situ data by Bea and Arnold (1973) and are tabulated in Table 1. For this case the total bed thickness is infinite. The design storm wave condition is; $T = 14$ s, $L = 152.4$ m, $H = 4.52^m$, and $h = 13.5^m$. The bottom pressure amplitude calculated from the linear wave theory is $p_o = 1.91 \times 10^4$ N/m^2.

The vertical distributions of the horizontal displacement, the vertical displacement of the soil and the wave induced pore pressure are shown in Fig. 7. Although the total bed thickness is infinite, a large horizontal displacement of 2.2 m exists at the mud line contrary to the case of homogeneous infinite bed. The pore pressure is maximum and equal to 1.7 KN/m^2 at z = 20 m. Therefore, the weak sublayer experiences large horizontal displacements and large pressure fluctuations. The stress distribution is shown in Fig. 8. As can be seen, large stresses penetrate deep in the seabed under the wave crest. Assuming the failure limit of the soils $\phi_f = 25^o$, the top portion of the bed up to 12 m below the mud line fails from the wave loading. Since the mud line is sloped in this area, the wave induced stress instability is predicted to induce a massive continuous landslide which causes toppling od bottom based platforms and pipeline failures as has happened during hurricane "Camille" in 1969.

PROTECTION OF SEABEDS BY CONCRETE BLOCKS AND RUBBLES

Stabilizing effects of concrete blocks and natural rubbles on the seabed response to waves are considered in this section. The present theory is applied to the problem of concrete blocks or rubbles placed on the seabeds to protect them from wave actions. The geotechnical properties of the sand used in the calculation are: $k = 10^{-4}$ m/s, $G = 10^7$ n/m^2, $\nu = 0.3$, $n = 0.3$, $d = 30$ m and $G_s = 2.7$. The seabed is on an impermeable and rigid bed, and the water depth is 10 m. The soil responses to the wave of $T = 8$ s,

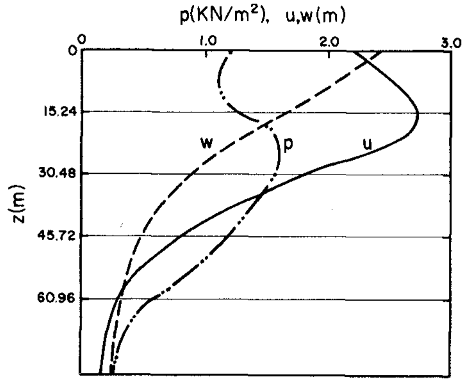

Figure 7. The vertical distributions of the horizontal displacement, u, the vertical displacement, w, of the soil and the wave induced pore pressure, p, in the Mississippi Delta clay seabed.

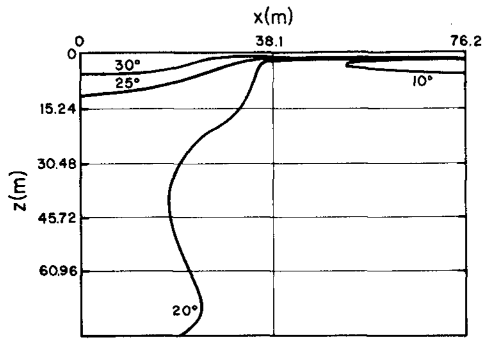

Figure 8. The distribution of the effective stresses in terms of stress angle ϕ in the Mississippi Delta clay seabed.

$H = 4$ m and $L = 71$ m are shown in Figs. 9 and 10. Figure 10 shows the distribution of the stress angle between the wave crest and the wave trough. (The crest exists at $x = 0$ and the wave propagates to the left). The distribution of the stress angle for $x < 0$ is again almost the same as this. Figure 10 shows that if the internal friction of the sand is 40^{o}, the penetration depth of failure zone is maximum at a wave crest and about 1.5 m. Therefore, the sandbed will fail in the failure zone and may cause liquefaction and sliding of the bed.

In order to protect the seabed from wave action, concrete blocks may be placed on it. The amplitudes of the soil displacements and pore-water pressure, and the distributions of the stress angle for the seabed covered by blocks of 3.0 m in thickness are shown in Figs. 11 and 12. The physical properties are: $G = 10^{8}$ N/m^{2}, $k = 1.0$ m/s, $\nu = 0.4$, n, $= 0.4$, $G_s = 2.2$. It can be seen from Fig. 9 and Fig. 11 that the amplitudes of soil displacements and pore-water pressure are hardly influenced by the blocks placed on the seabed. However, the distributions of the stresses shown in Fig. 12 become much smaller than those in Fig. 10. This is due to an increase in vertical and horizontal effective stresses by the weight of concrete blocks.

As discussed above, it has been verified theoretically that covering over seabeds by blocks is effective to protect them from waves. The optimal properties of the blocks can also be determined by using the theory.

We have also analyzed the effectiveness of the asphalt mats laid under the blocks. However, the results for such seabeds are similar to those shown in Figs. 11 and 12, and no additional effectiveness is noticed from the numerical results. It is predicted from the numerical results that the seabeds will fail from the storm waves and continuous landslides may result in the top portion of the bed 12 m from the mud line without a concrete block layer.

The numerical calculations suggest that such liquefaction and sliding of the seabed from waves can be prevented by placing a layer of concrete blocks or rubbles.

SUMMARY AND CONCLUSIONS

The response of multi-layered poro-elastic beds to water waves has been treated analytically in this paper. The number of layers, the thicknesses of the layers and geotechnical properties of the soil in each layer can all be aribtrary. The theory has been verified by the data of wave induced pore pressures from *in situ* measurements at the offshore area of the Mississippi River Delta by Bennett and Faris (1979).

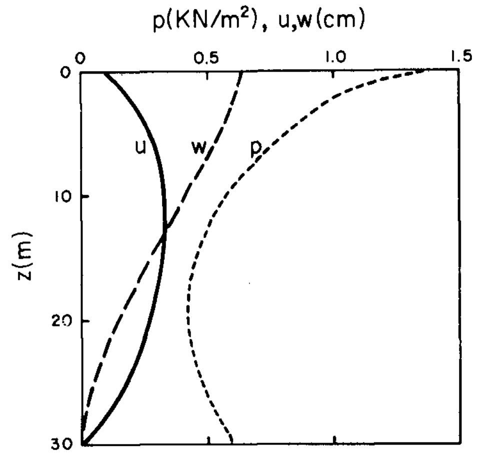

Figure 9. The vertical distribution of the horizontal displacement, u, the vertical distribution, w, and the wave inducec pore pressure, p, the the seabed without a concrete block layer.

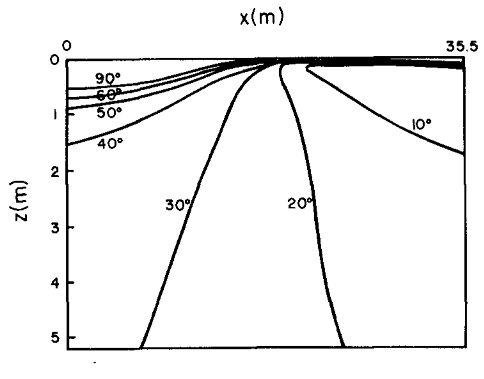

Figure 10. The distribution of the effective stresses in terms of the stress angle ϕ in degrees in the seabed without a concrete block layer.

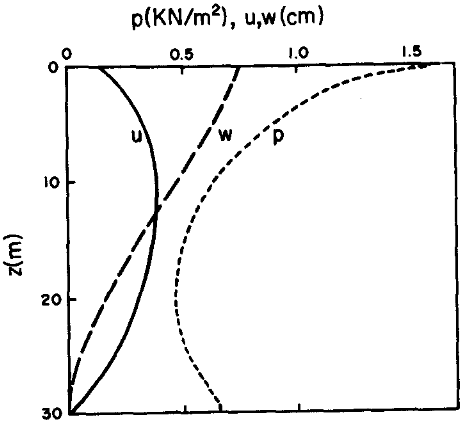

Figure 11. The vertical distribution of the horizontal displacement, u, the vertical distribution, w, and the wave induced pore pressure, p, in the seabed with a concrete block layer.

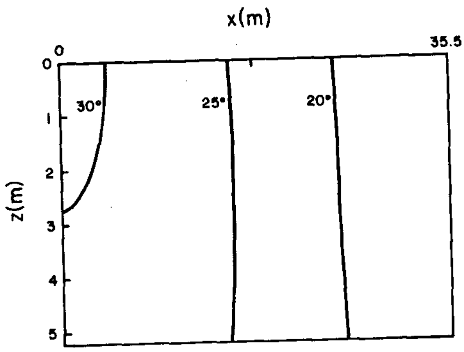

Figure 12. The distribution of the effective stresses in terms of the stress angle, ϕ, in the seabed with a concrete block layer.

The theory has been applied to the problem of the seabed response to the design waves at the North Sea. The theoretical results indicate that, for a given wave condition, there exists a critical bed thickness, $d = 0.20$ L, which creates the most unstable stress state in a homogeneous seabed. It has been indicated that generally the seabeds at the North Sea become unstable from large storm waves due to the relatively thin thickness of the seabeds.

As an example of inhomogeneous seabeds, the response of the soft clay beds with "crust profile" in offshore area of the Mississippi River Delta has been analyzed under attack of design storm wave. The numerical results indicate that large soil displacements, pore pressure fluctuations and stresses are induced by waves in the crust layer and the weakly consolidated sublayer below the crust.

The numerical results indicate that such wave induced stress instabilities can be prevented by covering the bed by a layer of concrete blocks and rubbles.

ACKNOWLEDGEMENTS

This work was entirely supported by the National Science Foundation, Grant No. CME 8009528. The authors are grateful for the support. The authors also wish to thank Dr. Richard Bennett for providing the pore pressure data and consultation on the structure of the submarine sediment.

REFERENCES

1. Bea, R. G. and Arnols, P., 1973. "Movements and forces developed by wave-induced slides in soft clays," Preprints of Offshore Technology Conference, OTC1899, Houston, Texas, May.

2. Bennett, R. and Faris, J., 1979. "Ambient and dynamic pore pressures in fine-grained submarine sediments in Mississippi Delta," Applied Ocean Research, Vol. 1, No. 3, pp. 115-123.

3. Biot, M. A., 1941. "General theory of three-dimensional consolidation," Journal of Applied Physics, Vol. 12, pp. 155-164.

4. Biot, M. A., 1955. "Thoery of elastically and consolidation for a porous anisotropic sold," Journal of Applied Physics, Vol. 26, No. 2, pp. 182-185.

5. Dawson, T. H., 1978. "Wave propagation over a deformable sea floor," Ocean Engineering, Vol. 5, pp. 227-234.

6. Madsen, O. S., 1978. "Wave-induced pore pressures and effective stresses in a porous bed," Geotechnique 28, No. 4, pp. 377-393.

7. Mei, C. C., and Foda, M. A., 1980. "Wave-induced responses in a fluid-filled poro-elastic soil with a free surface-A boundary layer theory," to be published.

8. Scott, R. F., 1963. "principles of soil mechanics," Addison-Wesley Publishing Company, Massachusetts.

9. Seed, H. B., and Rahman, M. S., 1978. "Wave-induced pore pressure in relation to ocean floor stability of cohesionless soils," Marine Geotechnology, Vol. 3, No. 2, pp. 123-149.

10. Yamamoto, T., 1977. "Wave-induced instability in seabed," Proc. of ASCE Spec. Conf., Coastal Sediments '77, pp. 898-913.

11. Yamamoto, et al., 1978. "On the response of the poro-elastic bed to water wave," Journal of Fluid Mechanics, Vol. 87, Part 1, pp. 193-206.

TABLE 1. The values of geotechnical properties of soils at the Mississippi Delta are used in numerical calculations.

Layer	1	2	3	4	5
d (m)	15.24	15.24	15.24	15.24	∞
k (m/s)	1×10^{-6}	1×10^{-6}	1×10^{-6}	1×10^{-6}	1×10^{-6}
G (N/m^2)	8×10^4	3×10^4	8×10^4	2×10^5	1×10^6
ν	0.45	0.45	0.45	0.45	0.45
n	0.3	0.3	0.3	0.3	0.3
γ_s	2.7	2.7	2.7	2.7	2.7
c (N/m^2)	8×10^3	3×10^3	8×10^3	2×10^4	1×10^5